

Spin transport through nanostructures

B. KRAMER^{1*}, K. DITTMER¹, S. DEBALD¹, J. OHE¹,
F. CAVALIERE^{1,2}, M. SASSETTI²

¹Institut für Theoretische Physik, Universität Hamburg, Jungiusstraße 9, 20355 Hamburg, Germany

²INFM-Lamia, Dipartimento di Fisica, Università di Genova, Via Dodecaneso 33, 16146 Genova, Italy

The influences of non-Fermi liquid correlations and spin-orbit scattering on the transport properties of quantum nanostructures connected to interacting leads are studied. Signatures of the spin are investigated in the transport. One-dimensional quantum dot is studied in the sequential tunnelling regime using the master equation approach. Quantum coherent conductance is calculated using the transfer matrix method for a quasi-one dimensional system with the Rashba coupling Hamiltonian, and for a two-dimensional quantum dot in a multi-terminal geometry modelled by the Ando Hamiltonian. In the sequential tunnelling regime, states with a higher total spin can be stabilized by suitably adjusting bias and gate voltages. Spin polarized current can be achieved by locally applying a magnetic field. For coherent linear transport through a multi-terminal device at zero magnetic field, we find a spin polarized current at certain energies, induced by spin-orbit scattering.

Key words: *spin transport; nanostructures; quantum dot; Rashba coupling*

1. Introduction

Transport properties of nanostructures related to the charge of the electron have been extensively studied during the past two decades, since the discovery of the conductance quantisation of quantum point contacts and two-dimensional electron systems in a quantising magnetic field, and of the Coulomb blockade in quantum dots connected to conducting leads by high tunnel barriers^{**}. The latter can be used to construct a single electron transistor (SET), in which switching between non-conducting and conducting states is done essentially with a single charge.

Transport phenomena in nanostructures related to the spin of the electron have attracted considerable interest only during the past few years^{***}, after the theoretical

*Corresponding author, e-mail: kramer@physnet.uni-hamburg.de.

**Overviews of the field can be found in Ref. [1].

***Some recent overviews can be found in Ref. [2].

proposal of a “spin transistor” [3]. Central issue of such a device is the possibility of producing a spin-polarized current that can be controlled by external means. In analogy to the SET device, the ultimate spin device could be imagined as a “single spin transistor” (SST), which would be switched between an “on-state” and “off-state” with a single electron spin. The discoveries of the spin blockade in sequential transport through quantum dots due to spin selection rules [4] and spin charge separation [5, 6] were important steps for achieving such a goal.

The standard way to generate a spin-polarized current is to inject electrons into a semiconductor from a ferromagnet [7], where it can be subsequently influenced by gate voltages. This is not very efficient due to scattering at the interface. The spin polarization is very small and there is also an accompanying charge current. Theoretically, several means of obtaining spin-polarized currents in nanostructures based on spin-orbit coupling have been discussed [8–13]. They are based on the fact that spin-orbit interaction has a polarizing effect on the quantum mechanical scattering of particles [14].

In the present paper, we address two issues. First, we investigate the control of spin in sequential transport through quantum dots in the presence of electron correlations. We show that by suitably adjusting source-drain voltage and the heights of tunnelling barriers one can stabilize states with higher total spin in a quantum dot. These states can lead to a negative differential conductance. By Zeeman splitting, one can achieve a spin polarization of the current, enhanced by electron correlation [15]. Differential spin conductance is strongly enhanced in the region of a higher spin state. Secondly, we study possibilities of achieving spin-polarization without using an external magnetic field. We find that in the presence of spin-orbit scattering, individual scattering states in low dimensional quantum nanostructures, such as quantum wires and quantum dots, can have spatially modulated spin polarizations. In non-equilibrium, such as is realized by linear dc current flow, the spatial modulation of the spin polarization of the states can lead to a polarization of the current. This happens when the Fermi energy is adjusted near the energy of a scattering state with a specific spatial polarization pattern and current and voltage probes are suitably attached to the nanostructure.

2. Spin blockade in sequential tunnelling

In this section, we summarize the theory of sequential transport through quantum dots in the presence of correlations, taking electron spin into account.

2.1. The Hamiltonian of a quantum dot with correlated electrons

For studying the interplay between spin polarized sequential tunnelling and correlations, we consider a one-dimensional quantum dot of length a , described as a Luttinger liquid, connected to non-interacting leads [15]. The Hamiltonian is (adopted units are such that $\hbar = 1$)

$$H_0 = \sum_{\nu=\rho,\sigma} \sum_q \omega_\nu(q) b_\nu^\dagger(q) b_\nu(q) + \frac{E_\rho}{2} (n - n_g)^2 + \frac{E_\sigma}{2} (s - s_B)^2, \quad \nu = \rho, \sigma \quad (1)$$

The first two terms take the collective charge ($\nu = \rho$) and spin ($\nu = \sigma$) density waves into account with the creation and annihilation operators b_ν^\dagger and b_ν , respectively. Here, n and s represent the total number of charges and the z -component of the total spin (units $\hbar/2$) of the electrons in the quantum dot, respectively. The total charge and spin are defined with respect to the average background values $\langle n \rangle = N_0$ and $\langle s \rangle = 0$, and are constrained by even $n + s$. The third term represents the energy necessary in order to change the charge n in the dot. An external gate voltage V_g has been incorporated into the Hamiltonian via the charge induced by the gate voltage $n_g e = C_g V_g$, with C_g being the gate capacitance and $-e$ the electron charge. The fourth term is analogous to the third one, and describes the energy needed to change the total spin s . An external magnetic field B induces a Zeeman splitting of $-g_B \mu_B B$, where g_B is the Landé factor and μ_B is the Bohr magneton. This in turn induces an effective average “spin number”

$$s_B = \frac{g \mu_B B}{E_\sigma} \quad (2)$$

which is the ratio between the Zeeman splitting and the spin addition energy E_σ . Note that the roles of n_g and s_B are very similar, as the last two terms in Eq. (1) describe the energy contributions due to charge and spin addition. Their physical origins, however, are very different. The charge addition energy is due to classical Coulomb repulsion, whereas the spin addition energy is a consequence of the Pauli principle [16] and is present in a system of finite size even without interaction.

2.2. Energy scales

An eigenstate of the Hamiltonian (1) can be represented by a state vector

$$|j\rangle = \left| n, s, \{l_q^\rho\}, \{l_q^\sigma\} \right\rangle \quad (3)$$

with $\{l_q^{\rho,\sigma}\}$ being the integer occupation numbers for a charge and spin collective mode. The energy of such a state can be written in terms of addition and excitation energies [15, 6]

$$U = \sum_q \left[l_q^\rho \omega_\rho(q) + l_q^\sigma \omega_\sigma(q) \right] + \frac{E_\rho}{2} (n - n_g)^2 + \frac{E_\sigma}{2} (s - s_B)^2 \quad (4)$$

The dispersion relation of the collective modes is linear due to the liberalization of the free spectrum around the Fermi level and to the assumption of short-range interactions

$$\omega_v(q) = \frac{v_F}{g_v} q \quad (5)$$

where v_F is the Fermi velocity. The parameters g_v parameterise the electronic interactions, g_ρ^{-2} being essentially the spatial average of the interaction potential. Here we neglect the exchange interaction, assuming a SU(2) spin invariance, such that $g_\sigma = 1$. For a noninteracting system $g_\sigma = 1$, while for repulsive interactions $g_\rho < 1$. A linear spectrum of the collective modes gives rise to a constant level spacing of charge and spin density waves

$$\varepsilon_\rho = \frac{\pi v_F}{a g_\rho}, \quad \varepsilon_\sigma = \frac{\pi v_F}{a} \quad (6)$$

The two remaining energy scales are the charge and spin addition energies E_ρ and E_σ , respectively. The charge addition energy

$$E_\rho = \frac{\pi v_F}{2 a g_\rho^2} \quad (7)$$

is strongly renormalized by the repulsive interactions between the electrons. On the other hand, spin addition is given by the noninteracting level spacing

$$E_\sigma = \frac{\pi v_F}{2 a} \quad (8)$$

As mentioned above, this energy scale is basically a result of the Pauli principle. In the model presented above, many physical effects affecting E_ρ have been disregarded, such as coupling with the external gates or a nearby 2D electronic gas. Such effects can lead to significant deviations from (7). Therefore, we will treat E_ρ as a free parameter in what follows.

2.3. Sequential transport

We assume that the quantum dot is connected via tunnelling barriers (H_t) to noninteracting left (L) and right (R) leads ($H_{L,R}$), which are kept at the chemical potentials μ_L and μ_R , respectively. The bias voltage applied to the quantum dot is $eV = \mu_L - \mu_R$. The total Hamiltonian is

$$H = H_0 + H_t + H_L + H_R \quad (9)$$

We assume very large left and right tunnelling resistances, $R_{L,R} \gg R_K = h/e^2$. We also assume that the excited *collective* states in the quantum dot relax instantaneously to the ground state. With this assumption, it is still possible to tunnel into an excited state. Since the relaxation time of the collective excitations is assumed to be much faster than any other time scale of the system, however, it is not possible to tunnel out of the quantum dot via such a state. In contrast, states with additional charge and/or spin are assumed to be stable. Therefore, the states of the dot that are relevant for transport can be labelled by the number of charges n and spin s alone, by the vector $|n, s\rangle$. We study transport in the sequential tunnelling regime, with tunnelling through left and right barriers being independent. The time-dependent occupation probabilities of the states in the quantum dot, $P_{|n,s\rangle}(t)$, satisfy the master equation

$$\partial_t P_{|n,s\rangle}(t) = \sum_{\lambda=L,R} \sum_{n'=n\pm 1} \sum_{s'=s\pm 1} \left[P_{|n',s'\rangle} \Gamma_{|n',s'\rangle \rightarrow |n,s\rangle}^{(\lambda)} - P_{|n,s\rangle} \Gamma_{|n,s\rangle \rightarrow |n',s'\rangle}^{(\lambda)} \right] \quad (10)$$

with the tunnelling rates Γ determined in the lowest order of perturbation theory for H_t [6]. For low temperatures, $k_B T \ll E_\sigma$, they have the form

$$\Gamma^{(\lambda)}(\Delta E) = \Gamma_0^{(\lambda)} \sum_{l_\rho=-\infty}^{\infty} \sum_{l_\sigma=-\infty}^{\infty} a_{l_\rho}^\rho a_{l_\sigma}^\sigma \gamma(\Delta E + l_\rho \varepsilon_\rho + l_\sigma \varepsilon_\sigma) \quad (11)$$

where

$$\Gamma_0^{(\lambda)} = \frac{2\omega_C}{e^2 R_\lambda} \left(\frac{\varepsilon_\sigma}{\omega_C} \right)^{1/2} \left(\frac{\varepsilon_\rho}{\omega_C} \right)^{1/2 g_\rho} \quad (12)$$

Here, ω_C is a cut-off frequency and $\Delta E \equiv E_f - E_i$ is the energy associated with a particular transition between an initial and a final state. We have defined the Fermi function for the leads as

$$\gamma(x) = \frac{1}{1 + e^{\beta x}} \quad (13)$$

with $\beta = 1/k_B T$. The weights $a_{l_\rho}^\rho$, $a_{l_\sigma}^\sigma$ arise from the density of states in the quantum dot. In the low temperature regime considered here, they are

$$a_{l_\rho}^\rho = \frac{\Gamma(1/2 g_\rho + l_\rho)}{\Gamma(1/2 g_\rho) l_\rho!}, \quad a_{l_\sigma}^\sigma = \frac{(2l_\sigma - 1)!!}{2^{l_\sigma} l_\sigma!} \quad (14)$$

where $\Gamma(x)$ represents the Euler gamma function. In the stationary limit, the left hand side of Eq. (10) is zero. The normalized probability distribution $P_{|n,s\rangle}$ is given by the

solution of a linear system of equations, with $\sum_{n,s} P_{|n,s\rangle} = 1$. We define the current for spin-up (+) and spin-down (-) electrons as

$$I_{\pm}(V) = e \sum_{n,s} \sum_{\Delta s = \pm 1} P_{|n,s\rangle} \left[\varphi_{\pm} \Gamma_{|n,s\rangle \rightarrow |n+1,s+\Delta s\rangle}^{(R)} - \varphi_{\mp} \Gamma_{|n,s\rangle \rightarrow |n-1,s+\Delta s\rangle}^{(R)} \right] \quad (15)$$

where $\varphi_{\pm} = (1 \pm \Delta s)/2$. The charge conductance is given by the derivative of the total current $I_{\rho} \equiv I_{+} + I_{-}$ with respect to the bias voltage

$$G_{\rho}(V, n_g, s_B) = \frac{\partial I_{\rho}}{\partial V} \quad (16)$$

The transport of spin is described by the spin-polarized current, $I_{\sigma} = I_{+} - I_{-}$, with a corresponding differential spin conductance

$$G_{\sigma}(V, n_g, s_B) = \frac{\partial I_{\sigma}}{\partial V} \quad (17)$$

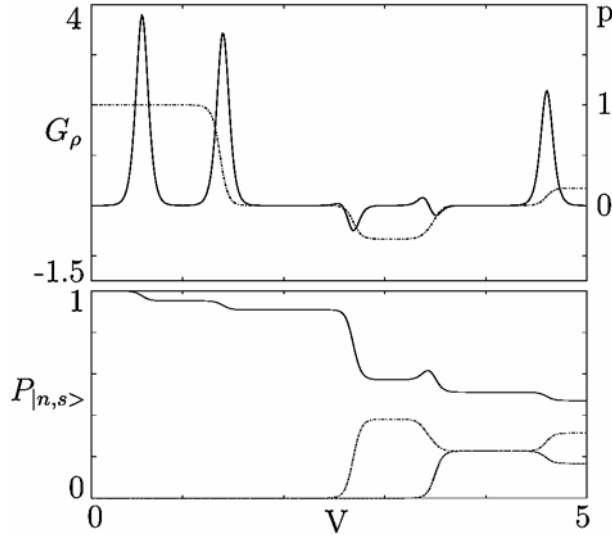


Fig. 1. Top: Differential conductance G_{ρ} (solid line, units $e^2 \Gamma_0^{(R)}$) and spin polarization p (dash-dot line) as a function of V (units E_{σ}/e) along the dotted horizontal line in Fig. 3 (top), with $n_g = 0.5$. Bottom: the corresponding stationary occupation probabilities $P_{|n,s\rangle}$ for $|n,0\rangle$ (solid line), $|n,2\rangle$ (dash-dot line), and $|n,-2\rangle$ (dashed line). The small probabilities $P_{|n+1,\pm 1\rangle}$ are not displayed in this plot. Note, however, that the population of the states $|n+1,\pm 1\rangle$ gives rise to positive conductance peaks (top panel) near $V \approx 0.6$ and $V \approx 1.4$. The parameters are $g_{\sigma} = 1$, $g_{\rho} = 0.4$, $E_{\rho} = 25E_{\sigma}$, $s_B = 0.2$, $k_B T = 0.02E_{\sigma}$ and $R_R/R_L = 20$

Figure 1 shows the voltage dependences of $P_{|n,0\rangle}$, $P_{|n,2\rangle}$, and $P_{|n,-2\rangle}$ near a Coulomb blockade peak for a transition from even n to $n + 1$, the corresponding differential conductance, and the spin polarization $p \equiv I_\sigma/I_\rho$. Negative differential conductances occur when states with $s = \pm 2$ become occupied (Fig. 3).

Let us discuss the behaviour of the transport in more detail. Charge and spin density waves represent collective excitations of the system. These modes, however, are not the only excited states of the system. For instance, $|n = 2q, s = 2p, 0, 0\rangle$ (p and q are integers with $|p| \geq 1$) are excited states with $2p$ partially aligned spins, without collective excitations. At zero magnetic field, the total-spin up and total-spin down components are energetically degenerate, and separated from the ground state $|n = 2q, s = 0, 0, 0\rangle$ by $\delta E_p = 2p^2 E\sigma$. States with an odd number of electrons, $n = 2q + 1$, can be considered similarly. Here, the excited states with partially aligned spins have spin $|s| = 2p + 1$, ($p \geq 1$).

States with higher spins can be accessed in the non-linear transport regime. In order to relax to the ground state, the total spin has to be changed. This is not possible without spin-flip scattering processes, apart via a tunnelling event. Even in the presence of spin-flip processes it remains difficult to relax to an energetically lower state and simultaneously change the total spin [17]. It is thus reasonable to assume that, in contrast to internal collective excitations, excited states with higher spins do not intrinsically relax. Dynamical states are characterized by their total number of charges n and the total spin s .

Such high-spin states play an important role in the transport, particularly in systems with asymmetric barriers, as discussed below. At finite, non-zero magnetic fields, such states can become ground states of the system due to Zeeman splitting of the total-spin up and total-spin down components.

2.4. Results

In this section, we summarize some of the results obtained for sequential tunneling, including the identification of parameter regions for which high-spin states yield the dominant contributions to transport [6]. We also summarize some recent results on spin polarized differential conductivity in the presence of a magnetic field localized at the quantum dot. It appears that the contributions of higher-spin states can not only lead to negative differential conductances but also increase the differential spin conductance.

In the following, we concentrate on the region close to a resonance in the linear conductance. This is given by the condition that the chemical potentials in the left and right leads are the same as the chemical potential of the quantum dot, defined as the difference in the ground states of n and $n + 1$ electrons

$$\mu_d = E_\rho \left(n + \frac{1}{2} - n_g \right) + E_\sigma (\bar{s}_{n+1} - \bar{s}_n) \left[\frac{\bar{s}_n + \bar{s}_{n+1}}{2} - s_B \right] \quad (18)$$

with \bar{s}_n, \bar{s}_{n+1} being the spin of the ground state for $n, n + 1$ electrons, respectively. For a fixed n_g , the ground state of the dot can be found by minimizing the total energy (4) with respect to $n, s \in z$, with $l_q^\rho = l_q^\sigma \equiv 0$.

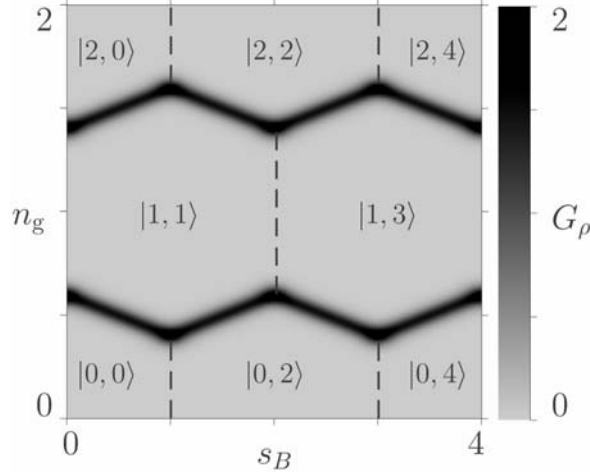


Fig. 2. Greyscale plot of the differential conductance G_ρ (units $e^2 \Gamma_0^{(R)}$) as a function of s_B and n_g for $V \rightarrow 0$. $E_\rho = 5E_\sigma$, $k_B T = 0.1E_\sigma$ and other parameters as in Fig. 1. In each region, the corresponding ground state $|n, \bar{s}_n\rangle$ of the dot is shown. Starting with small values of n_g , peaks for the transitions $n = 0 \leftrightarrow n = 1$ and $n = 1 \leftrightarrow n = 2$ appear. With increasing B , the states $|n+1, 1\rangle, |n, 2\rangle, |n+1, 3\rangle \dots$ successively become ground states of the quantum dot. This is indicated by the zigzag behaviour of the conductance peak positions as a function of s_B .

Figure 2 shows the linear conductance ($V \rightarrow 0$) in the plane of n_g and s_B . The zigzag behaviour of the peaks with increasing B is due to the fact that states with successively higher spins become ground states of the quantum dot.

With increasing voltage V , higher spin states can contribute to the transport. A scheme of the spin transitions near $|n, s\rangle \rightarrow |n+1, s \pm 1\rangle$, with n even and $0 < s_B < 1$, is shown in Fig. 3 together with numerical results for asymmetric barriers. When transitions to the state with $s = 2$ become possible, the latter accumulates transition probability at the expense of the states with $s = 1$ and $s = 0$ (Fig. 1). This leads to a negative differential conductance, indicated in the lower panel of the figure.

Figure 4 shows greyscale plots of the differential conductance G_ρ and spin conductance G_σ for asymmetric barriers ($R_R/R_L = 20$) in the plane of bias voltage V and magnetic field s_B , for a value of n_g in the Coulomb blocked region and n even, such that states with successively higher spins become ground states (cf. Fig. 2). For $V = 0$

(Fig. 4, top), we clearly observe the above-mentioned analogy between s_B and n_g . This is indicated by the equidistant conductance peaks at $s_B = 1/2, 3/2, 5/2, 7/2, \dots$ and the constant current regions between them. In these regions, spin states with higher spins $s_B = 1, 2, 3, 4, \dots$ become stabilized, in close analogy to the Coulomb blocked charge states along n_g at $V = 0$ for $s_B = 0$. As soon as higher spin states become occupied in the non-linear regime, the conductance becomes negative as mentioned earlier [5, 6].

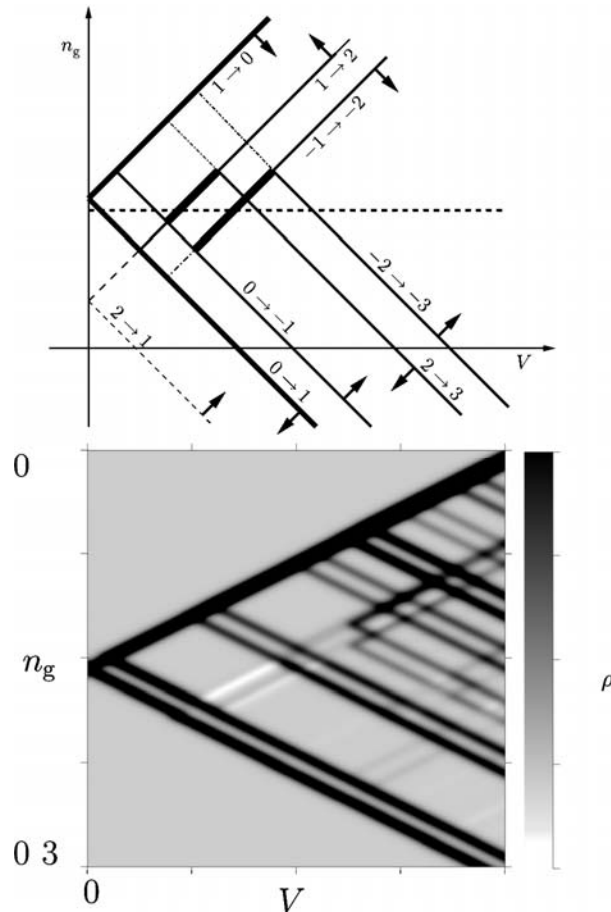


Fig. 3. Top: scheme of the possible transitions for sequential transport through a quantum dot, with $0 < s_B < 1$ in the plane of V (units E_d/e) and n_g , around the resonance between the states $|n, 0\rangle$ and $|n+1, 1\rangle$, for even n and low spin values. Each transition line is labelled by the spin involved. Dashed transition lines do not contribute to the differential conductance. Dash-dotted lines: transitions involving a spin density wave. Arrows: movement of the transition lines with increasing B . Horizontal dotted line: cut along which the conductance, current polarization and occupation probabilities are shown in Fig. 1. Bold lines: regions of negative differential conductance. Bottom: greyscale plot of the differential conductance (arbitrary units) for $k_B T = 0.1 E_{\sigma}$, and other parameters as in Fig. 1; black/white lines: positive/negative differential conductance

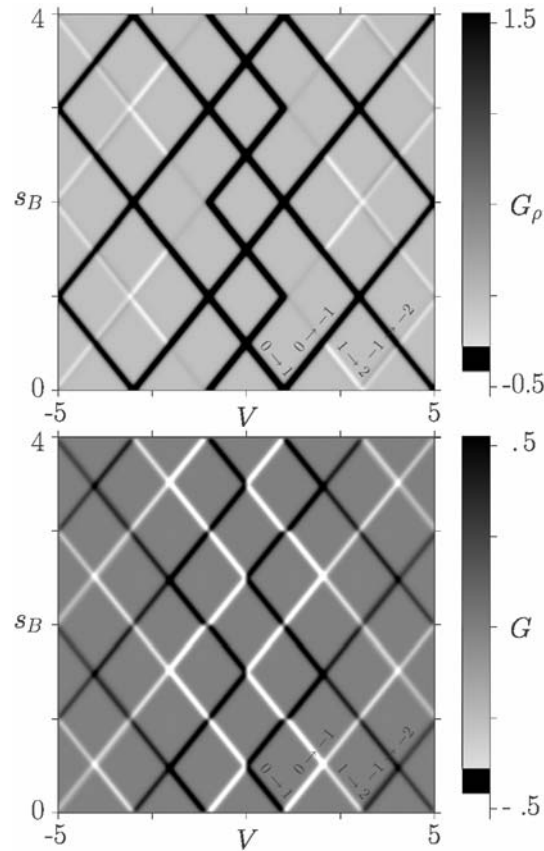


Fig. 4. Greyscale plots of differential conductances (units $e^2\Gamma_0^{(R)}/E_\sigma$) as a function of s_B and V (units E_σ/e), for $n_g = 0.5$ and even n , such that successively higher-spin states become ground states with increasing B ; parameters: $g_\sigma = 1$, $g_\rho = 0.4$, $E_\rho = 25E_\sigma$, $k_B T = 0.02E_\sigma$ and $R_R/R_L = 20$. Top: total conductance G_ρ ; starting with small values of s_B , for $V = 0$ equidistant conductance peaks occur at $s_B = 1/2, 3/2, 5/2, 7/2 \dots$ for the ground-state-to-ground-state transitions $|n, 0\rangle \leftrightarrow |n+1, 1\rangle$, $|n+1, 1\rangle \leftrightarrow |n, 2\rangle$, etc. Bottom: spin conductance G_σ ; exactly at $V = 0$, the spin conductance vanishes, since temperature is finite; spin conductance becomes large when the transition lines involved with higher spin states intersect

The behaviour of the spin conductance (Fig. 4, bottom) is the most interesting. The spin conductance vanishes for non-zero temperature exactly at zero bias voltage, since positive and negative spin conductances cancel around $V = 0$ in the temperature window given by $k_B T$. At the points where transition lines involving higher spins intersect, however, the spin conductance is enhanced. This is related to the fact that the spin polarization p changes from positive to negative at these points.

3. Spin polarization via spin-orbit interaction

In this section, we investigate the influence of spin-orbit scattering on transport through quantum wires and dots in the metallic regime, i.e. where resistance is of the order of resistance quantum, $R \approx h/e^2$. We will show that even without a magnetic field the current can become spin polarized, given the quantum structure is suitably contacted.

3.1. Spin-orbit Hamiltonian

In the inversion layer of heterostructures, spin-orbit interaction can be described in the effective mass approximation by the Rashba Hamiltonian [18]

$$H_R = \frac{1}{2m}(\vec{p} + e\vec{A})^2 + V(x, y) + \frac{1}{2}g\mu_B B\sigma_z - \frac{\alpha}{\hbar}[(\vec{p} + e\vec{A}) \times \vec{\sigma}] \quad (19)$$

Here, $\vec{p} = (p_x, p_y)$ is the momentum operator in the plane of the inversion layer, \vec{A} is the vector potential of the magnetic field $\vec{B} = (0, 0, B)$ perpendicular to the inversion layer, m is the effective mass, g is the Landé factor of the electron and $V(x, y)$ is an additional confining potential. The Rashba parameter α describes the average strength of the electric field, due to the asymmetric potential well confining electrons in the inversion layer at $z = 0$. In general, in addition to the Rashba term, there is also a band structure contribution [19], due to the absence of inversion symmetry. It can be neglected in InAs, in which Rashba spin-orbit interaction is strong.

For a zero magnetic field and no additional confinement, the Rashba Hamiltonian can be diagonalised. The energy eigenvalues are

$$E_{\pm} = \frac{\hbar^2}{2m}k^2 \pm \alpha k \quad (20)$$

and the corresponding eigenspinors

$$\psi_{1,2} = \begin{pmatrix} 1 \\ \pm e^{-i\varphi} \end{pmatrix} e^{i\vec{k} \cdot \vec{r}} \quad (21)$$

with $\vec{k} = (k_x, k_y)$, $\vec{r} = (x, y)$, $k_y = k \cos \varphi$, and $k_x = k \sin \varphi$. For a given energy, there are two wave numbers contributing to the propagation of the particle. This has two important consequences. First, the spin rotates upon propagation in a given direction. A spin-up state at $x = 0$ will be converted into a spin-down state at $x \pi/\Delta k \equiv \pi\hbar/2m\alpha$. This may be easily seen by considering one-dimensional propagation in the x -direction. Second, when a plane wave with a given wave vector and energy is re-

flected from a hard wall, say along the x -direction, the reflected wave consists of partial waves with different x -components of the wave vector. This implies that there is a spatial modulation of the spin polarization, which depends on the incidence angle of the plane wave. This is a special case of a general result in quantum mechanical scattering theory, namely that the spin polarization of the scattering wave function of a strong spin-orbit scatterer is spatially modulated [14]. Generally, this is simply a consequence of the spin *not* being a good quantum number due to the spin-orbit scattering term in the Hamiltonian. It should be emphasized that in equilibrium, without a magnetic field, this does not yield any spin polarization. Since the Hamiltonian is time reversal invariant, such that Kramers degeneracy remains intact, each energy corresponds to two degenerate states, which have exactly opposite spin polarizations. In the above example of Rashba states, these degenerate are the states with opposite wave vectors.

3.2. Spin polarization in a quantum wire

As a more detailed illustration, we consider the states in a quasi-one dimensional system described by Eq. (19), along the y -direction with a symmetric confinement $V(x) = V(-x)$ and $B = 0$. In this case, the Hamiltonian commutes with p_y and the unitary operator

$$U_x = P_x \sigma_x \quad (22)$$

where P_x is the inversion operator for the x -coordinate. Without spin-orbit interaction, P_x and σ_x are conserved separately. The operator U_x is called spin parity. This symmetry is broken for $B \neq 0$.

Spin parity symmetry at $B = 0$ has two consequences. First, there is a degeneracy of the energy spectrum at $k = 0$, even without Zeeman splitting. This degeneracy disappears for $B \neq 0$, which yields a quantisation of the dc conductance, in units of e^2/h instead of $2e^2/h$, as a function of the Fermi energy. The latter is significantly different from that due to simple Zeeman splitting of the subbands (Fig. 5). For large B , the splitting of energy bands converges towards spin split Landau levels.

Second, at $B = 0$, spin-parity invariance $[H, U_x] = 0$ implies, for the components of an eigenspinor of the Hamiltonian

$$\psi(x, y) = e^{ik_y y} \begin{pmatrix} \psi^\uparrow(x) \\ \psi^\downarrow(x) \end{pmatrix} \quad (23)$$

the symmetry property

$$\psi^\uparrow(x) = \pm \psi^\downarrow(-x) \quad (24)$$

This, for the *local* spin density in a given eigenstate, in general yields

$$\sigma_z(x) = |\psi^\uparrow(x)|^2 - |\psi^\downarrow(x)|^2 = |\psi^\uparrow(x)|^2 - |\psi^\uparrow(-x)|^2 \neq 0 \quad (25)$$

since P_x alone is not a symmetry operation. The average spin density vanishes for $B = 0$, but $\langle \sigma_z \rangle \neq 0$ for $B \neq 0$. Also, due to Kramers degeneracy, the local spin density at a given energy vanishes for $B = 0$, since there is a second, time-reversed state, corresponding to the wave vector $-k_y$ if the former had k_y , with exactly the opposite polarization.

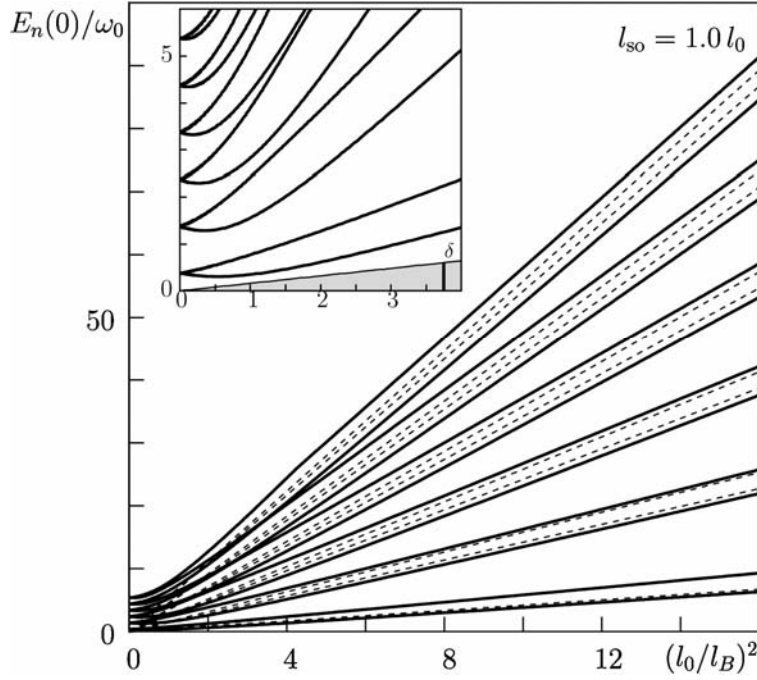


Fig. 5. The lowest twelve eigenenergies of a quantum wire at $k = 0$ as a function of the magnetic field, for $l_{SO} = l_0$ and typical InAs parameters: $\alpha = 1.0 \times 10^{-11}$ eVm, $g = -8$, and $m = 0.04m_0$. Dashed lines: a fan of Landau levels $\hbar\omega_c(n+1)/(n+1/2) \pm \delta/2$; inset: results for low fields; shaded region: bulk Zeeman splitting δ

In order to obtain a non-zero polarization at a given energy, time reversal symmetry has to be broken. This can normally be achieved by applying a magnetic field or by magnetic scattering.

3.3. The conductance of a spin-orbit scatterer

Even without a magnetic field, however, the time reversal symmetry can be broken, namely by injecting a current into the system and thus generating a stationary

non-equilibrium state. This can be done in a transport experiment. Quantum mechanically, this corresponds to a scattering experiment in which an incoming wave with wave number \vec{k} is scattered. The stationary scattering wave function, corresponding to a *given* wave vector, will thus exhibit a spatial modulation of the spin polarization for a spin-orbit scatterer. If such a wave function is then locally probed, it should be possible to detect local spin polarization.

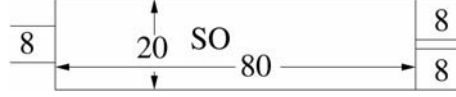


Fig. 6. The fork-shaped three-terminal device used for calculating the quantum conductance shown in Fig. 7. The conductance is measured between the left and uppermost right contacts

In nanostructured quantum systems, such local probing can be achieved by contacting the system and performing a dc-transport experiment. Theoretically, this can be done by calculating the conductance via the Landauer formula

$$G = \frac{e^2}{h} \text{Tr} t^\dagger t \quad (26)$$

with t being the transmission matrix of the scatterer.

For numerical purposes, it is convenient to use the corresponding tight binding Hamiltonian [20] instead of Eq. (19). On a two dimensional lattice with (l,m) points and a lattice constant a

$$H = V \sum_{lm} \begin{pmatrix} \cos \theta & i \sin \theta \\ i \sin \theta & \cos \theta \end{pmatrix} |lm-1\rangle \langle lm| + \begin{pmatrix} \cos \theta & -\sin \theta \\ \sin \theta & \cos \theta \end{pmatrix} |l-1m\rangle \langle lm| + h.c. \quad (27)$$

where $V(\cos \theta (= \hbar^2/2ma^2))$ is the energy unit, and the angle θ describes the spin-orbit scattering. This angle can be related, via the discretisation of Eq. (19), to the parameter α according to

$$\tan \theta = \frac{ma\alpha}{\hbar^2} \quad (28)$$

Numerical results for the spin-resolved conductance of a rectangular quantum dot attached to three quantum wires (Fig. 6) are shown in Fig. 7. Current flows from the contact on the left hand side to the contact on the upper right. The predicted strong spin polarization due to spin-orbit scattering of the conductance is clearly observed at certain Fermi energies.

4. Conclusion

In this contribution, we have discussed several features of the transport properties of quantum dots related to electron spin. Two transport regions have been considered. In sequential transport, we have described features related to the occupation of correlated many-electron states with higher total spins, namely the spin blockade phenomena that lead to negative differential conductance in the non-linear transport regime. We have seen that these higher spin states also give rise to strong differential spin conductances in the presence of a magnetic field in the quantum dot.

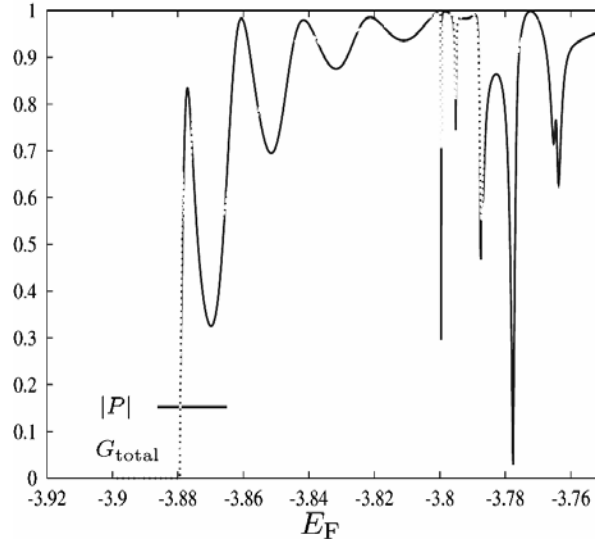


Fig. 7. The linear total conductance (dashed, units e^2/h) and the spin polarization $\bar{P} = \text{Tr}(t^\dagger \bar{\sigma} t) / G_{\text{total}}$ (full line) as functions of the Fermi energy of a rectangular quantum dot connected to three leads in the geometry of a fork

Furthermore, we have considered a spin-orbit scatterer in the quantum coherent metallic regime. We have argued that scattering states exhibit a spatial modulation of spin polarization. When time reversal invariance is broken, this can be used to generate a spin-polarized current, even when no magnetic field is applied and no magnetization is present. It has been argued that such a situation can be achieved in stationary non-equilibria such as a dc-transport experiment.

The effects discussed here might be of importance for designing a pure-semiconductor based spin transistor.

Acknowledgments

This work was supported by the EU via contracts FMRX-CT98-0180 and HPRN-CT2000-00144, and by the Deutsche Forschungsgemeinschaft via SFB 508 of the Universität Hamburg and the

Graduiertenkolleg *Nanostrukturierte Festkörper*. Useful discussions with Stefan Kettmann, Tobias Brandes, and Tomi Ohtsuki are gratefully acknowledged.

References

- [1] *Quantum transport in semiconductor submicron structures*, B. Kramer (Ed.), NATO ASI Ser. E 326, Kluwer Acad. Publ., Dordrecht, 1996; *Semiconductor quantum structures*, B. Kramer (Ed.), Landolt-Börnstein, New Series, Group III, Vol. 34, Subvol. B, Part 1, *Quantum point contacts and quantum wires*, Springer Verlag, Berlin 2001; *Mesoscopic Electron Transport*, L.L. Sohn, L.P. Kouwenhoven, and G. Schön (Eds.), Kluwer Acad. Publ., Dordrecht, 1997.
- [2] *Semiconductor spintronics and quantum computation*, D.D. Awschalom, D. Loss, N. Samarth (Eds.), Springer Verlag, Berlin, 2002; WOLF S.A., AVSCHALON D.D., BUHRMAN R.A., DAUGHTON J.M., VON MOLNÁR S., ROUKES M.L., CHTCHELKANOVA A.Y., TREGER D.M., *Science*, 294 (2001), 1488.
- [3] DATTA S., DAS B., *Appl. Phys. Lett.*, 56 (1990), 665.
- [4] WEINMANN D., HÄUSLER W., KRAMER B., *Phys. Rev. Lett.*, 74 (1995), 984.
- [5] CAVALIERE F., BRAGGIO A., STOCKBURGER J.T., SASSETTI M., KRAMER B., *Phys. Rev. Lett.*, 93 (2004), 036803.
- [6] CAVALIERE F., BRAGGIO A., SASSETTI M., KRAMER B., *Phys. Rev. B*, 70 (2004), 125323.
- [7] BRATAAS A., NAZAROV YU.V., BAUER G.E.W., *Phys. Rev. Lett.*, 84 (2000), 2481.
- [8] BRUNO P., *Phys. Rev. Lett.*, 79 (1997), 4593.
- [9] PAREEK T.P., BRUNO P., *Phys. Rev. B*, 63 (2001), 165424.
- [10] KISELEV A.A., KIM K.W., *Appl. Phys. Lett.*, 78 (2001), 775.
- [11] DITTMER K., Diplomarbeit, Universität Hamburg, 2004.
- [12] PAREEK T.P., *Phys. Rev. Lett.*, 92 (2004), 076601.
- [13] KHODAS M., SHEKHTER A., FINKELSTEIN A.M., *Phys. Rev. Lett.*, 92 (2004), 086602.
- [14] LANDAU L.D., LIFSHITZ E.M., *Theoretical Physics*, Vol. 3, *Quantum Mechanics*, Pergamon Press, Oxford, 1980.
- [15] BRAGGIO A., SASSETTI M., KRAMER B., *Phys. Rev. Lett.*, 87 (2001), 146802.
- [16] KLEIMANN T., SASSETTI M., KRAMER B., YACOBY A., *Phys. Rev. B*, 62 (2000), 8144; KLEIMANN T., CAVALIERE F., SASSETTI M., KRAMER B., *Phys. Rev. B*, 66 (2002), 165311.
- [17] KHAETSKII A.V., NAZAROV YU.V., *Phys. Rev. B*, 61 (2000), 12639.
- [18] RASHBA E.I., *Fiz. Tverd. Tela*, 2 (1960), 1224 (*Sov. Phys. Sol. State*, 2 (1969), 1109); BYCHKOV YU.A., RASHBA E.I., *Pis'ma Zh. Eksp. Teor. Fiz.*, 39 (1984), 66 (*Sov. Phys. JETP Lett.*, 39 (1984), 78).
- [19] DRESSELHAUS G.F., *Phys. Rev.*, 100 (1955), 580.
- [20] ANDO T., *Phys. Rev. B*, 40 (1989), 5325.

Received 5 November 2004

Revised 10 November 2004